[3] Influence of the discreteness of synthetic and digital holograms on their imaging properties

S.N. Koreshev [1], D.S. Smorodinov [1], O.V. Nikanorov [1]
[1]St. Petersburg National Research University of Information Technologies, Mechanics and Optics, St. Petersburg, Russia

Abstract

We study in which way the discreteness of synthetic and digital holograms affects their imaging properties, i.e. the structure and quality of the image under restoration. We establish and substantiate requirements to the relationship between the basic parameters of synthesis or recording of a discrete hologram - operating wavelength, the angle of incidence of the reference wave, the size of the minimal object feature, and the hologram sampling period to ensure the matching between the object structures and the reconstructed image. We also examine the possibility of easing these requirements, provided either by modifying the structure of the hologram, or using a frequency substitution effect, characteristic of the discrete structures.

Keywords: *holography, synthetic hologram, digital hologram, discrete structure, imaging properties, method of representation, binarization.*

Citation: *Koreshev SN, Smorodinov DS, Nikanorov OV. Influence of the discreteness of synthetic and digital holograms on their imaging properties. Computer Optics 2016; 40(6): 793-801. DOI: 10.18287/2412-6179-2016-40-6-793-801.*

Introduction

Fast development of digital and computer equipment in the last few years has caused growing interest of the optical electronic hardware researchers and developers in synthetic and digital holograms.

Synthetic holograms are generally understood as holograms calculated by computer and hardcopied with image generators. Digital holograms on the other hand are registered in the coherent light with CCD sensors or other electronic devices. Nevertheless both types of holograms are basically similar to each other and are distinguished from conventionally recorded ones by their discrete structure.

Current literature provides quite good coverage of the hologram synthesis. For example, [1-3] describe the methods to synthesize the holograms suitable for practical photolithography applications when the object is usually a two-dimensional transparent overlay. In the general case, they essentially calculate the holographic field intensity in each hologram dot and plane under different synthesis parameters [4], such as wavelength used, distance between hologram and object, size of the smallest object structure element, etc.

Meanwhile the particular properties of imaging by discrete holograms or in other words their imaging capabilities have not been studied in the sufficiently detailed way. Whereas understanding such particulars is a crucial factor since it facilitates optimization of hologram synthesis and reconstruction in terms of hardware and time resources used. These were the factors behind writing this paper, which is aimed at researching the imaging properties of discrete diagrams as applicable to synthesized hologram projectors used for projection holographic photolithography.

1. Imaging Properties of Discrete Holograms

Impact of the discrete hologram structure on the reconstructed image

The most convenient way to investigate the discrete hologram imaging properties is to start with analyzing the spatial spectrum of the field reconstructed with the discrete hologram of field $U_d(\xi)$ [5]:

$$U_d(\xi) = t_0 F\left\{r\exp(2\pi i\xi_r x)\right\} - kF\left\{r\exp(2\pi i\xi_r x)\right\} \otimes \left\{\left(\begin{bmatrix} F\left\{A(x)A^*(x)\right\} + F\left\{r^2\right\} + \\ +F\left\{A(x)r\exp(-2\pi i\xi_r x)\right\} + \\ +F\left\{A^*(x)r\exp(2\pi i\xi_r x)\right\} \end{bmatrix} \otimes \sum_{n=-N}^{N}\delta(\xi-\xi_n)\right) \otimes a(\sin(\pi\xi a)/\pi\xi a)\right\}. \quad (1)$$

The analysis shown in this paper was conducted for the discrete amplitude hologram of a two-dimensional transparent overlay object, generated by the object wave propagating along the line normal to the synthesis plane, or by registering the hologram and reference wave falling at a certain angle to it (off-axis or Leith&Upatnieks hologram [6]). Selection of this particular research object would not interfere with the generality of the results obtained, since the amplitude modulation of hologram would affect only its linearity and diffraction efficiency but would not sufficiently change the hologram imaging properties predetermined by its discreteness.

The first summand of equation (1) describes the amplitude of radiation reconstructed by the continuous hologram registered in the analog form. The second summand is a convolution of the equation describing the spectra of zero and first orders of analog hologram diffraction with the sum of unit-impulse functions. It describes periodic repetition of the spectrum of the field reconstructed with the continuous hologram predetermined by the discrete structure of the hologram.

Thereat the multiplication period of this spectrum is equal to $\xi_n = 1/d_d$, where d_d – is the period of hologram discretization. Note also that the second summand of equation (1) includes the product of multiplied spectrum times the function depending of the value $\sin(\varpi\xi a)$, which is the evidence of modulation of the reconstructed field spectrum. In case of the synthesized hologram, this modulation is defined by the diameter of the focal spot of the image generator, or the fill factor of the CCD sensor in case of digital hologram. Note that the spatial frequency of reconstructing wave corresponds to the maximum of this modulating function.

Spectrum of the amplitude of the field reconstructed by discrete hologram is schematically displays on Figure 1 [7, 8]. The object here is characterized by the spatial frequency band of $\pm\Delta/2$. 2Δ wide peaks on this schematics are intermodulation interference. Narrower peaks of Δ width correspond to the spectra of the images reconstructed in the first orders of the hologram diffraction. Unit-impulse functions shown as arrows on the diagram describe periodic repetition of the reconstructing wave spectrum caused by the discrete structure impact.

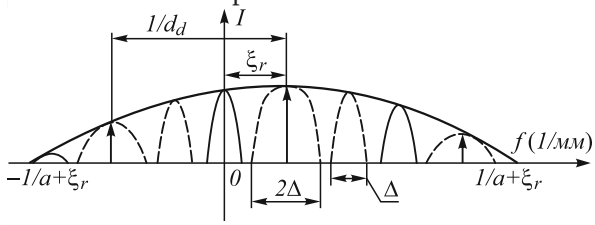

Fig. 1. Spectrum of the field reconstructed with the discrete structure hologram

The spectrum shape shows the presence of specific conditions that permit to select the optimal hologram synthesis (or registration) parameters in terms of ensuring spatial separation of the reconstructed field components. For example, if we select the hologram sampling period equal to the focal area diameter of the image generator in use (CCD-sensor pixel):

$$a = d_d, \tag{2}$$

then the envelope line nodes will mate with the position of multiplied spectra of the reconstructing wave, which will result in suppressing the reconstructing wave spectrum multiplication. Meanwhile the requirement for spatial separation of all components of the reconstructed field remains in force, which demands artificial limitation of the registered object spectrum width. Such limitation may be recorded as an inequation:

$$\Delta \le 1/4d_d. \tag{3}$$

Hence, it is possible to define the requirement to the spatial frequency of the reference wave. It must be equal to:

$$|\xi_r| = \sin|\theta|/\lambda = 1,5\Delta_{\max}, \tag{4}$$

where $\Delta_{\max} = d_d/4$. The condition for selecting the optimum angle of incidence of the reference wave follows from equation (4):

$$\sin|\theta| = 1,5\lambda/4d_d. \tag{5}$$

(5) results in a new limitations for the operating wave length used to reconstruct the discrete hologram. Since the value of $\sin|\theta|$ cannot exceed 1, the wave length suitable to reconstruct the synthetized hologram may not exceed the value of the hologram sampling period more than 2.7 times.

Equation (3) that correlates the object spectrum width with the hologram sampling period, permits to infer the limitations of the object maximum spatial frequency $\xi_{o\max}$, arising due to its discrete structure:

$$|\xi_{o\max}| = \Delta_{\max}/2 = 1/8d_d. \tag{6}$$

Whereas (6) leads to limitation of minimum size of object structure element a_t, which is related to the hologram discrete structure:

$$a_t \ge 1/2|\xi_{o\max}| = 4d_d. \tag{7}$$

Taking into account (7) it follows from (5) that the minimum size of the object element shall not be less than 1.5λ to guarantee spatial discrimination of all diffraction orders. However even in this case the hologram will register only the sideband of the object spectrum. Successful registration of the entire object spectrum will require registering the information in the frequency band of:

$$\xi_{\max} \le 2\Delta_{\max} = 4\left|\xi_{o\max}\right|. \quad (8)$$

Using the sustained progressing wave condition [3], we can infer the following equations from (8):

$$4\left|\xi_{o\max}\right|\lambda \le 1, \quad (9)$$

$$\left|\xi_{o\max}\right| \le 1/4\lambda. \quad (10)$$

Hence, it follows that provided the hologram diffraction orders spatial separation is maintained the entire object spectrum may be registered on the discrete hologram only when the following inaquations are satisfied:

$$a_t \ge 2\lambda \text{ and } d_d \ge \lambda/2. \quad (11)$$

Also note that subject to diffraction limitations the minimum size of the image structure element used in the optic science is equal to the wave length λ. Consequently, the hologram discrete structure would result in at least sesqui-fold or even two-fold size increase of the minimum element of the reconstructed image.

Impact of the discrete holograms structure modification on the hologram imaging properties

Since most of discrete holograms processing occur in the virtual space it becomes possible to modify their structure in some way to improve their imaging properties [8, 9]. For example, decreasing the function that describes the holographic field intensity distribution by the squared module of the object field amplitude makes is possible to eliminate the intermodulation interference from the field reconstructed with a discrete hologram [10]. After such modification the following equation will describe intensity distribution *I'* in the hologram synthesis or registration plane:

$$I' = r^2 + 2ar\cos\left(\phi_a - \phi_r\right). \quad (12)$$

This modification significantly affects the structure of the spectrum of the reconstructed field and will shape it in a way shown on Figure 2. It is evident that the central peaks corresponding to intermodulation interferences are gone. The object allowable spectrum width is increased which permits to reduce the optimal angle of reference wave incidence and the allowable size of the discrete hologram pixel. Possible contrasting distortions in the reconstructed images caused by the structure changes are negligible in this case since the objects in questions are binary.

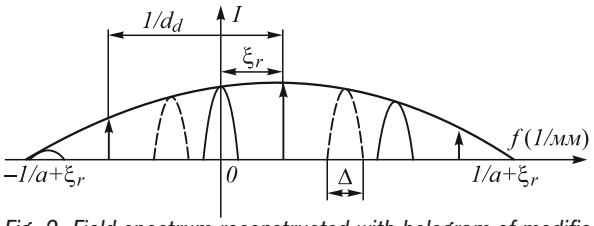

Fig. 2. Field spectrum reconstructed with hologram of modified discrete structure

Correctness of the established equations are confirmed by experiments where several holograms of the same test object were synthesized (Figure 3).

The following hologram synthesis parameters were selected subject to the established requirements and used to perform research described in this paper: operating wave length λ = 13.5°μm; size of the object structure minimum element (1 pixel) a_t = 80°μm; distance between object and hologram planes R_h = 20345°μm; hologram sampling period d_d = 20°μm; angle of flat reference wave incidence θ = 14.67°. Meanwhile the value of the reference wave incidence angle and the hologram structure type (with or without the modification described above) were changing in the course of this research.

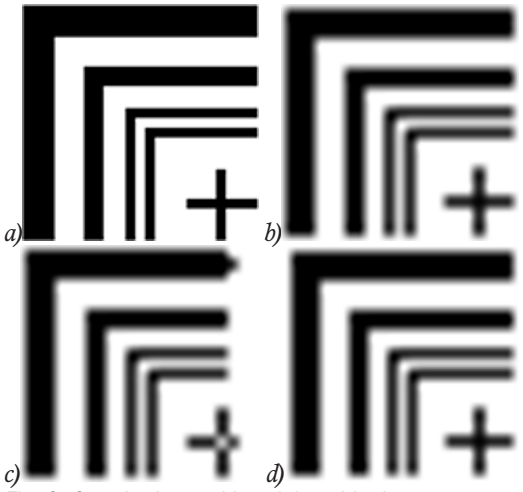

Fig. 3. Standard test object (a) and its images reconstructed with a hologram, recorded at the design estimated angle of reference wave incidence of θ = 14.7⁰ (b); at the reduced angle of θ = 9.7⁰ without structure modification (c) and with the modified structure (d). Images are after threshold processing

Also note that all experiments mentioned in this paper were performed using a specialized software package developed by Applied and Computer Optics Department of the Saint Petersburg National Research University of Information Technologies, Mechanics and Optics. This package is designed to synthesize and digitally reconstruct hologram projectors [4].

The research results shown on Figure 3 demonstrate that when the incidence angles of the reference and reconstructing waves do not satisfy equation (5) it is impossible to reconstruct the image of the structure identical to the object structure using the synthesized hologram. Meanwhile hologram modification has permitted to reduce the allowable angle of the reference wave incidence.

The modification under review is useful primarily for registration of digital holograms of binary objects, since the CCD sensors used for this purpose generally have low resolving power. Changing the incidence angle of the reference wave permits to reduce spatial frequency of the registered holographic structure, which can ensure successful registration of hologram with sufficiently large size of CCD sensor pixel.

Frequency substitution effect for recording and reconstruction of discrete holograms

One more feature of discrete holograms should not be ignored. The fact is that the discrete structure of digital and synthesized hologram results in so-called effect of substitution or masking of the registered spatial frequencies [10, 11].

When digital holograms are recorded this effect manifests itself in the following way: the sensor detector recognizes high spatial frequencies as lower frequencies within the maximum allowable Nyquist frequency equal to $|F_n| = 1/2d_d$, where d_d – signal sampling time:

$$\xi_r = 2mF_n + \xi = 2m/2d_d + \xi. \qquad (13)$$

Here ξ_r is the spatial frequency of the registered holographic structure; ξ – difference of special frequencies ξ_r and $2mF_n$; $2m$ – quotient from division of registered spatial frequency ξ_r by Nyquist frequency F_n, rounded up or down to the nearest whole number.

This paper's findings include that such effect can be used to register low frequency digital holograms under large angle of reference wave incidence when the object is located on the normal to the registration plane. If the hologram spatial frequency is deemed to satisfy equation (4), then formula (13) can be translated as follows:

$$\frac{\sin\theta'}{\lambda} = \frac{m}{d_d} \pm \frac{\sin\theta}{\lambda}, \qquad (14)$$

where θ – small angle of reference beam incidence defined based on Nyquist criterion; θ' – increased beam convergence angle; λ – operating wave length; $m = 0,1,2...$ Hence, follows the equation for the allowable values of reference beam incidence angle:

$$\theta' = \arcsin\left(\sin\left(\theta\right) \pm m(\lambda/d_d)\right). \qquad (15)$$

This condition may be useful when the hologram cannot be registered at the reference wave incidence angle defined as per (5) due to structural limitation of the registration installation.

Note that the frequencies substitution effect is manifested not only when registering digital holograms, but also when reconstructing synthesized holograms, which makes it possible to reconstruct them under the reconstructing beam incidence angle larger than the reference beam incidence angle used for synthesis.

2. Synthesized Hologram Imaging Properties Behavior and the Object Representation Method

Since the synthesized holograms have discrete structure, certain assumptions related to the impact of this structure need to be applied for calculation of the complex amplitude distribution. As a result, the actual description of the distribution of complex amplitude of object wave in the object plane obtained under the assumptions will consist of a certain array of discrete counts. The holographed object must have the discrete structure to ensure successful synthesis, therefore it can be said that actually the synthesis handles the discrete hologram of a discrete object. Hence, the parameters used for the object discretization, or its representation method, cannot but have a certain impact on the imaging properties of synthesized holograms [12].

Subject to equation (11) successful reconstruction of the discrete object image would require that the synthesized hologram sampling period must be at least 4 times less than the sampling period of the object itself. The same value is accepted as the center-to-center distance between adjacent dots to form the synthesized hologram.

But the research has shown that when the photosensitive resists or optical sensors used have high resolution, i.e. their pixel size is smaller than a_t, this method of object representation is hardly suitable for practical applications. It should be also noted that using the reconstructed image sensors with the pixel size below a_t to reconstruct the synthesized holograms would not affect the minimum pixel size displayed in the reconstructed image. In strict compliance with (11) the reconstructed image pixel size is defined solely by the hologram sampling period and aperture and is equal to a_t.

Figure 4 shows the test object and its image reconstructed with different values of resolving power of photosensitive resist or CCD sensor used to register the image.

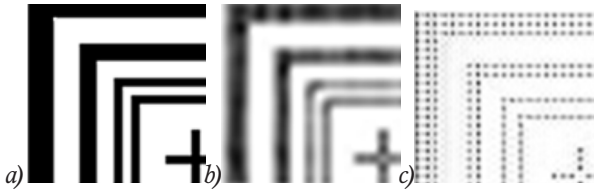

Fig. 4. Test object (a) and its image, reconstructed with different values of resolving power: standard (b), increased 4 times against standard value (c)

The images show that as long as the photosensitive resists resolving power does not exceed the dot size of the original object (this resolving power is called standard), the image is kept continuous, which means it is suitable for photolithographic process (Figure 4b). In the mean time when photosensitive resists with larger resolving power are used, the single image of the object is actually split into separate dots (Figure 4b).

This effect is caused by disruptions of synthesis of Rayleigh criterion according to which the dots that produce an image are perceived as separate in case the gap of intensity distribution of adjacent dots exceeds 22.5 % [6].

Accordingly, we can formulate the condition for selecting the object representation method for hologram synthesis that would ensure continuity of the reconstructed image. Therefore as per the Rayleigh criterion the center-to-center distance between adjacent dots must not exceed the Airy disk radius:

$$R_E = 1,22(\lambda/2A), \quad (16)$$

where λ – operating wave length, A – numerical aperture. Given that

$$A = \lambda/a_t, \quad (17)$$

where a_t – size of a separate dot as a minimum object elements, we obtain:

$$R_E = 0,61a_t. \quad (18)$$

Since the objects under examination are discrete, all relations between periods must be in multiples of two. Hence the overall requirement to the object sampling period which shall satisfy inequation:

$$R \le 0,5a_t. \quad (19)$$

According to (19) the hologram synthesis process shall include selecting the object sampling period, which is at least 2 times smaller than the value calculated based on the spatial frequency analysis results.

The research conclusions were confirmed by experiments. For these ends holograms of two objects were synthesized – standard test object and a two pixel wide vertical line. Different object sampling periods were used for synthesis – from 80 μm (design value) to 20 μm (4 times smaller than design value).

Figure 5 shows the images reconstructed with each of the holograms.

It follows from the experiment results that the best quality of the reconstructed image is achieved when the hologram projector synthesis uses the representation method with the object sampling period 4 times smaller than the optimal period based on (11).

In case of a complex object the difference between the second and third images are practically invisible; for simple objects minor differences still persist and are probably related to higher imaging precision requirements.

Therefore it has been established that high quality reconstruction of an image during hologram synthesis would require at least four counts of the transmission function of the object per each of the elementary resolvable fragments of its structure.

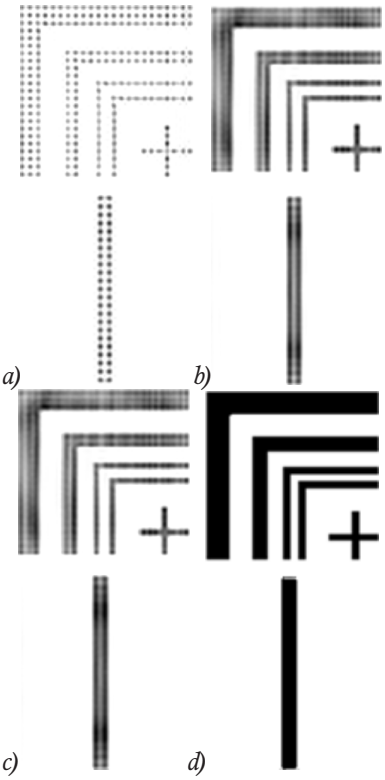

Fig. 5. Images of different objects obtained from reconstruction of holograms synthesized with object sampling periods (dot p diameter) of: a) 80 μm; b) 40 μm; c) 20 μm; d) 20 μm, after threshold processing. Size of the image detector resolving cell: 10 μm

3. Binarization of Synthesized Holograms and its Impact on the Reconstructed Image Quality

Binary structure is another important feature of synthesized holograms suitable for practical applications. The point is that the computer synthesized hologram is

a half-tone transparent overlay consisting of 256 gray shades [13]. Meanwhile special laser image generators are used to transfer such hologram onto a physical media. Currently such generators are able to ensure accurate transfer of only two tones of amplitude transmission factor [14]. This requires binarization of synthesized hologram, which in turn further affects its imaging properties. The hologram is usually binarized at the upper threshold subject to the selected binarization level *t*, which value falls in the range from 0 to 256. Generally, the object can consist of elements of various sizes. Hence the selected binarization level must ensure that after image reconstruction and threshold processing no object elements are distorted, i.e. that their intensity levels are approximately the same. Research was performed to establish the relation between the reconstructed image intensity and the original object size. This research included comparing the intensity of two reconstructed objects – a single dot and a rectangle sized $m \times n$ dots.

The intensity of i_{mn} rectangle image would depend on the ratio between the areas of original object S_0 and the S_{mn} hologram aperture section, and also on the diffraction efficiency of this section η_{mn}. It can be defined as follows:

$$i_{mn} = (S_{mn}/S_0)\eta_{mn}. \quad (20)$$

If we assume the dot object intensity as equal to i_p, and the diffraction efficiency of the corresponding hologram section as η_p, we can determine the ratio of diffraction efficiencies required to ensure equal intensity of the reconstructed images of two objects [15]:

$$\frac{\eta_{mn}}{\eta_p} = \frac{m^2 n^2 \left(2\lambda R_h + a_t^2\right)^2}{\left(2\lambda R_h + a_t^2 mn\right)^2 + 2\lambda a_t^2 R_h \left(m-n\right)^2}. \quad (21)$$

The available literature report that the diffraction efficiency of reflective discrete binary relief-phase hologram is defined by the values of the wave length, relief height and pulse ratio, interrelated with the following equation [16]:

$$\eta = (4/\pi^2)\sin^2(\pi S)\cdot\sin^2((2/\lambda)\pi h), \quad (22)$$

where S – hologram pulse ratio, h – hologram relief height. If we assume that the relief height selected is optimal in terms of achieving maximum diffraction efficiency of reflective relief-phase holograms, and is equal to $\lambda/4$ [4], so the appearance of (22) is improved:

$$\eta = (4/\pi^2)\sin^2(\pi S). \quad (23)$$

Subject to (23) it seems that if the fixed relief height and wave length values are assumed the binary hologram pulse ratio *S* is the only parameter that affects its diffraction efficiency value. Meanwhile the selected level of hologram binarization directly affects the pulse ratio value. Figure 6 illustrates the holographic field intensity distribution of the hologram of two different-sized object prior to binarization.

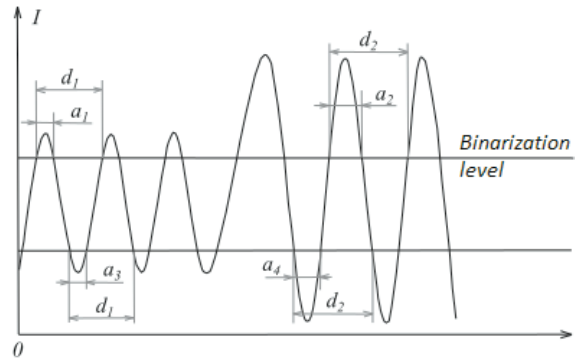

Fig. 6. Holographic field intensity distribution of two object of different area. Relation between pulse ration and binarization level is shown

If such hologram is binarized at the level highlighted on the figure with the top line, the pulse ratio of two aperture sections of the obtained binary hologram S_1 and S_2 will be equal to, correspondingly:

$$S_1 = a_1/d_1 \text{ and } S_2 = a_2/d_2, \quad (24)$$

where d_1 and d_2 – local spatial periods of the hologram. Based on the completed research and relatively weak dependence between S_2 and S_1 pulse ratio values and the selected hologram binarization level, conclusion may be deduced as of the impact of the hologram binarization level selection on the relative intensity of the images reconstructed with such hologram. Thereunder in order to produce an image closest to the original object in terms of the intensity distribution, the optimal for this purpose hologram binarization level must be selected. As shown on Figure 6, there are generally two levels of this kind.

The relation between quality of reconstructed images of differently sized objects and binarization level of the synthesized hologram projectors will be illustrated experimentally. Figure 7 shows reconstructed images of a standard test object, obtained with different hologram projectors.

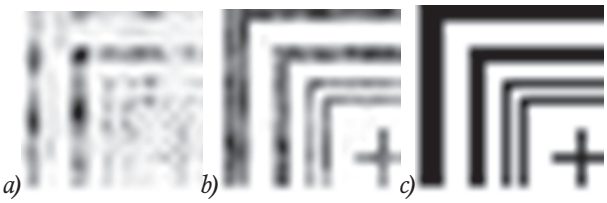

a) b) c)

Fig. 7. Test object images reconstructed with the holograms binarized at medium binarization level (a) and at optimal level: before (b) and after (c) threshold processing

The first of these two holograms (Figure 7a) was synthesized at the medium binarization level of 128, which is equal to the half of the maximum intensity. The second

hologram binarization level (Figure 7b) was determined experimentally in terms of smoothing the intensity between differently sized elements of the reconstructed images; this binarization level is equal to 87.The second optimum level for this object hologram is equal to 56.
After threshold processing the image reconstructed with the hologram binarized at the optimal level completely matches the original object (Figure 7c), while the image on Figure 7a is virtually destroyed.

4. Synthesis of Hologram Projectors Designed to Reconstruct Three-Dimensional Images

Characteristics of synthesized holograms imaging performance permit to generate images on the curved surfaces, which can be used in photolithographic process among other things [17]. The non-planar object may be represented as an aggregate of two-dimensional amplitude transparent overlays parallel to the hologram synthesis plane at various distances from the hologram so that the geometric center of each overlay is considered to be located on the normal reconstructed from the center of hologram. The spacing between adjacent transparent overlays in the resulting set must not exceed the hologram depth of field. Such spacing would permit to use a set of standard planar holograms to emulate recording of the hologram intended to reconstruct non-planar (three-dimensional) image.
The simplest object of such type is two parallel transparent overlays located at different distances from the hologram plane (Figure 8).

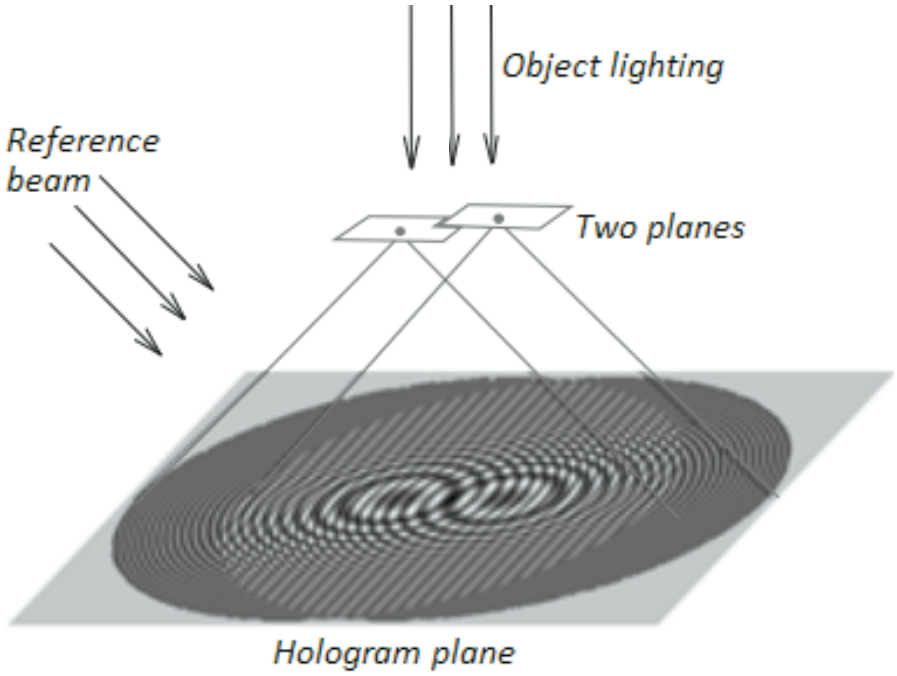

Fig. 8. Generation of hologram of non-planar object

Meanwhile the image depth of field cannot exceed the value defined by the following equation [18]:

$$b = \pm(\lambda n / 2A^2), \quad (25)$$

where A – numeric beam aperture; λ – operating wave length; n – refractive index of the media between hologram and photographic mask ($n = 1$ for air). The following equation defines the numeric aperture of the radiation, diffracted at the smallest element of the photographic mask structure for this case of split-beam hologram with the flat reference wave falling at a certain angle against the hologram synthesis plane:

$$A = n \sin\alpha = \lambda / a_t. \quad (26)$$

Here a_t – is the smallest photographic mask structure elements, specifically the size of one pixel of the discrete hologram may be accepted for such value; α – aperture angle of the diffracted radiation.
Operability of the synthesis method of Frensel hologram projectors that generate the image on the curved surfaces was verified experimentally; for this purpose a number of hologram projectors were synthesized and reconstructed. Two virtual two-dimensional transparent overlays with an image of a standard test object were used and spaced at 100 to 500 μm at 100 μm steps. At standard synthesis parameters as per (25) the depth of field of the reconstructed image shall correspond to value $b = \pm 237$ μm. Each hologram was

reconstructed at two values of the distance between the hologram and the image recording plane h_1 and h_2, that define the best reconstruction of the corresponding transparent overlays that form a non-planar object. Figure 9 shows the research results.

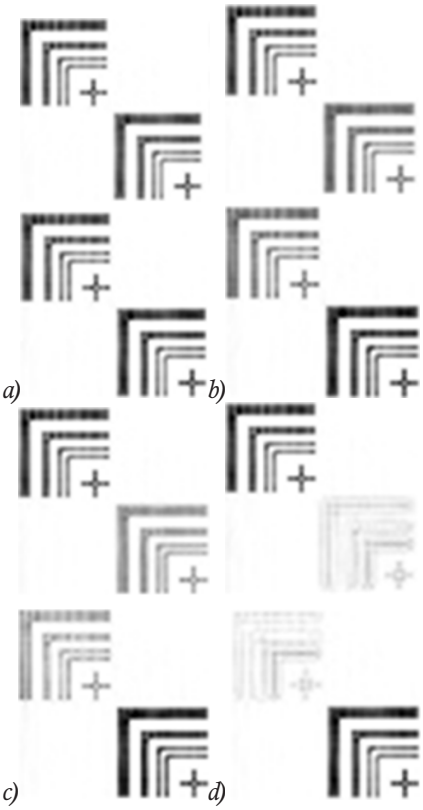

Fig. 9. An image in the recording plane at the distance of h_1 (top) and h_2 (bottom) with the distance between transparent overlays a) 100 μm from each other, b) 200 μm, c) 300 μm, d) 500 μm

As one can see both images are practically identical as long as the distance between the object does not exceed the depth of field during the synthesis (Figure 9 a, b). With larger distance, quality of one image deteriorates gradually (Figure 9 c) until it is completely destroyed (Figure 9 d).

Conclusion

In summary, this research work included complete examination of key imaging properties of discrete holograms. Requirements to the ratios between the following major hologram synthesis or recording parameters were established: reference wave angle of incidence , operating wave length λ, minimum size of the object structure element a_t, and hologram pixel size d_a. These ratios need to be satisfied to reconstruct high quality images with discrete hologram. Besides that, research covered possibility of the hologram structure modification to relax the established requirements, and possible practical application of specific discrete hologram properties such as frequency substitution effect. Methods of practical application of this effect were proposed.

Besides that, the research examined the impact of the object representation method and hologram binarization on its imaging properties. Examination covered peculiarities of synthesized holograms imaging properties as applied to photolithography on curved surfaces. The equations that permit to emulate the three-dimensional object hologram recording with a set of standard flat holograms were established and experimentally verified.

Results of experimental verification of all established theories were presented.

Acknowledgment

This work was partially supported by the Ministry of Education and Science of Russian Federation (Project 3.2506.2017/4.6**).**

References

1. Koreshev SN, Ratushnyj VP. Using the method of holography to obtain images of two-dimensional objects when solving problems of high-resolution photolithography. J Opt Techn 2004; 71(10): 673-679. DOI: 10.1364/JOT.71.000673.

2. Lesem LV, Hirsch PM, Jordan JA Jr. The kinoform: A new wavefront reconstruction device. IBM Journal of Research and Development 1969; 13(2): 150-155. DOI: 10.1147/rd.132.0150.

3. Collier RJ, Burkhardt ChB, Lin LH. Optical holography. Bell Telephone Laboratories; 1971.

4. Koreshev SN, Nikanorov OV, Gromov AD. Method of synthesizing hologram projectors based on breaking down the structure of an object into typical elements, and a software package for implementing it. J Opt Techn 2012; 79(12): 769-774. DOI: 10.1364/JOT.79.000769.

5. Koreshev SN, Nikanorov OV, Smorodinov DS. Imaging properties of discrete holograms. I. How the discreteness of a hologram affects image recontruction. J Opt Techn 2014; 81(3): 123-127. DOI: 10.1364/JOT.81.000123.

6. Landsberg GS. Optika [In Russian]. Moscow: "Fizmatlit" Publisher; 2003.

7. Koreshev SN, Semyonov GB. The diffraction efficiency and some of the features of the spectra of discrete holograms [In Russian]. Optics and Spectroscopy 1976; 41(2): 310-313.

8. Yaroslavsky LP, Merzlyakov NS. Methods of digital holography [In Russian]. Moscow: "Nauka" Publisher; 1977.

9. Zhang Y, Lu Q, Ge B. Elimination of zero-order diffraction in digital off-axis holography. Optics communications 2004, 240(4-6), 261-267. DOI: 10.1016/j.optcom.2004.06.040.

10. Koreshev SN, Smorodinov DS, Nikanorov OV. Imaging properties of discrete holograms. II. How structural modification of the holoram and a high spatial carrier frequency of the hologram structure that exceeds the Nyquist frequency affects the image re-

construction. J Opt Techn 2014; 81(4): 204-208. DOI: 10.1364/JOT.81.000204.

11. Khovanova NA, Khovanov IA. Methods of analysis of time series [In Russian]. Saratov: "GosUNTs Kolledzh" Publisher; 2001.

12. Koreshev SN, Smorodinov DS, Nikanorov OV, Gromov AD. How the method of representing an object affects the imaging properties of synthesized holograms. J Opt Techn 2015: 82(4): 246-251. DOI: 10.1364/JOT.82.000246.

13. Johnson S. Stephen Johnson on Digital Photography. O'Reilly Media, Incorporated; 2006. ISBN: 978-0-596-52370-1.

14. Slinger CW, Cameron CD, Coomber SD, Miller RJ, Payne DA, Smith AP, Smith MG, Stanley M, Watson PJ. Recent developments in computer-generated holography. Proc SPIE 2004; 5209: 27-41. DOI: 10.1117/12.526690.

15. Koreshev SN, Smorodinov DS, Nikanorov OV, Gromov AD. Intensity equalization for elements for binary-object images reconstructed using synthesized hologram projectors. Optics and Spectroscopy 2013; 114(2): 288-292. DOI: 10.1134/S0030400X13020136.

16. Koreshev SN. The diffraction efficiency of discrete binary phase holograms. Optics and Spectroscopy, 1978, 44(1), 39-42.

17. Koreshev SN, Smorodinov DS, Nikanorov OV, Gromov AD. Synthesizing hologram–projectors for photolithography on non-planar surfaces. J Opt Techn 2015; 82(2): 90-94. DOI: 10.1364/JOT.82.000090.

18. Shehonin AA, ed., Tsukanova GI, Karpova GV, Bagdasarova OV, Karpov VG, Krivopustova EV, Yezhova KV. Applied Optics. Part 2: Study Guide [In Russian]. Saint-Petersburg: "SPbGITMO (TU)" Publisher, 2003.